

# GENERATION OF MAGNETIC FIELDS FOR ACCELERATORS WITH PERMANENT MAGNETS

*T. Meinander*

Technical Research Centre of Finland, Espoo, Finland

## **Abstract**

Commercially available permanent magnet materials and their properties are reviewed. Advantages and disadvantages of using permanent magnets as compared to electromagnets for the generation of specific magnetic fields are discussed. Basic permanent magnet configurations in multipole magnets and insertion devices are presented.

## **1. INTRODUCTION**

Guiding of charged particles in accelerators is predominantly achieved with the aid of magnetic fields. There are three basic technologies for creating these fields: normal electromagnets, superconducting electromagnets and permanent magnets. Normal electromagnets are predominating at moderate field strengths (up to about 1.5 T), but in certain applications such fields can be created more favorably using permanent magnets and e.g. some short period undulator fields are impossible to generate with electromagnets. Superconducting magnets are employed for the generation of higher field strengths or for covering very large field volumes.

## **2. PERMANENT MAGNET MATERIALS**

Any ferromagnetic material with a large enough hysteresis to generate a useful field in the outside space after magnetization, can be utilized as a permanent magnet. Over the years a large number of such materials have been developed for different purposes. Today four basic classes of materials make up over 99 % of the permanent magnets produced [1]. All these materials have been discovered after 1930. Ordered chronologically according to discovery they are:

- i) Alnico, metallic alloys containing mainly iron, cobalt and nickel together with smaller amounts of aluminium, copper and titanium;
- ii) Hard ferrites, ceramic compounds of basic composition  $\text{BaO} \cdot 6\text{Fe}_2\text{O}_3$  or  $\text{SrO} \cdot 6\text{Fe}_2\text{O}_3$ ;
- iii) REC (rare earth-cobalt), which have two basic compositions,  $\text{SmCo}_5$  and  $\text{Sm}_2\text{Co}_{17}$ , but are available in a large variety of grades with part of the samarium replaced by other rare earths and other additives.
- iv) NEO (neodymium-iron-boron) with basic composition  $\text{Nd}_2\text{Fe}_{14}\text{B}$ , but also available in many grades with slightly different composition.

Typically the working point of a permanent magnet lies in the second quadrant of the main hysteresis loop, which is called the demagnetization curve. Figure 1 shows the demagnetization curves (both flux density and polarization are shown) of a modern high coercivity material from group iii or iv above. The most important parameters used for characterizing a permanent magnet material are also indicated. They are the remanence ( $B_r$ ), the energy product ( $(BH)_{max}$ ), the coercivity of the flux density ( $H_{cB}$ ) and the coercivity of the polarization ( $H_{cJ}$ ).

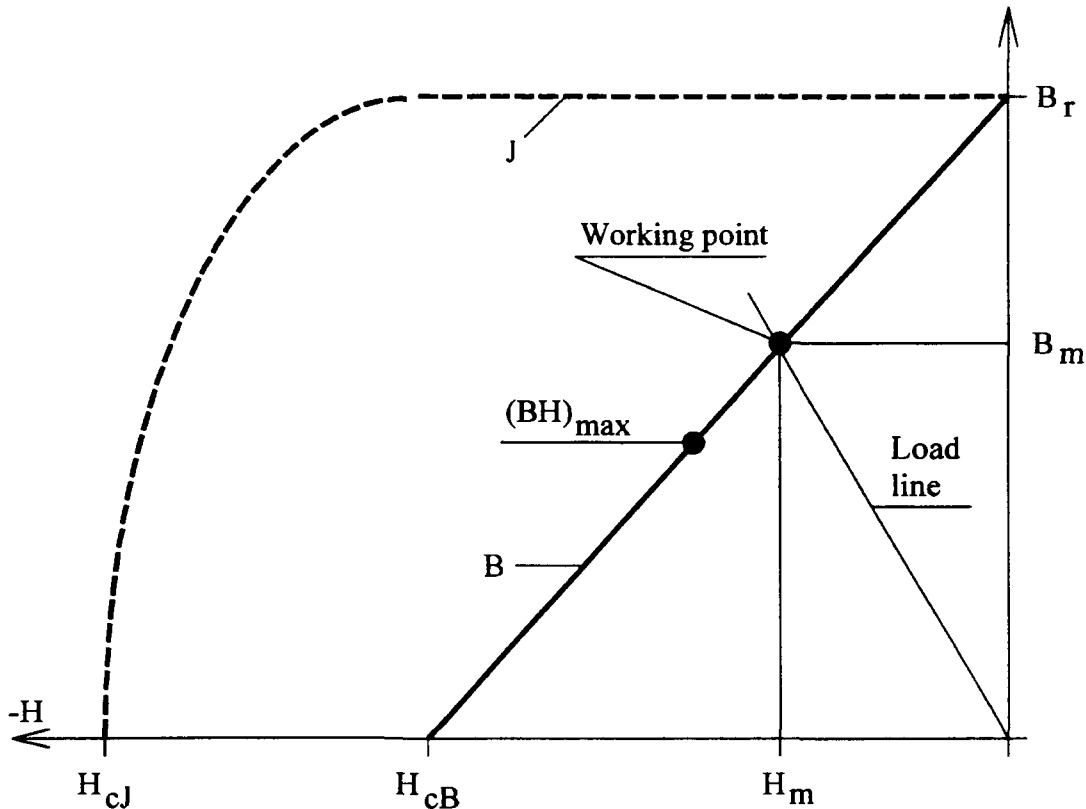


Fig. 1 The demagnetization curve and working point of a high coercivity permanent magnet material

Table 1 shows typical values of these parameters and some other important characteristics of high grade materials. Note that maximum values of all parameters cannot be achieved in the same material. The most typical trade-off is between  $B_r$  and  $(BH)_{max}$  on one hand and  $H_{cJ}$  on the other hand. Prices vary within large brackets depending on material grade and the size, shape, dimensional and magnetic tolerances, quantity and surface treatment of the blocks. The prices given in the table are "order of magnitude" averages given to show the great differences between the different classes of materials.

**Table 1**

Properties of permanent magnet materials. The values of the magnetic parameters are close to maximum values of commercial high grade materials.

	<b>Alnico</b>	<b>Ferrite</b>	<b>REC</b>		<b>NEO</b>
Composition	Fe-alloy	$\text{SrO} \cdot 6\text{Fe}_2\text{O}_3$	$\text{SmCo}_5$	$\text{Sm}_2\text{Co}_{17}$	$\text{Nd}_2\text{Fe}_{14}\text{B}$
$B_r$ (T)	1.3	0.4	0.9	1.1	1.2
Temp. coeff. of $B_r$	-0.02	-0.2	-0.06	-0.04	-0.12
$H_c$ (kA/m)	150	320	2400	2000	1400
$(BH)_{\max}$ (kJ/cm <sup>3</sup> )	50	25	170	250	300
Curie-point (°C)	800	450	750	800	300
Density (g/cm <sup>3</sup> )	7.2	5.0	8.2	8.4	7.4
Corrosion resistance	good	good	good	good	poor
Radiation hardness		good	good	good	adequate
Price (ECU/kg)	25	2.5	200	200	180

### 3. CALCULATION OF PERMANENT MAGNET FIELDS

Magnetic fields generated by permanent magnets - often together with an iron yoke and/or pole pieces - can be calculated with most of the finite difference and finite element computer codes originally developed for electromagnets. Permanent magnets are then characterized by their demagnetization curve and the direction of magnetization in the block. Finite element methods generally produce accurate and reliable results, but are time-consuming and tedious to use in the design and optimization of magnetic circuits, which require frequent changes of the configuration and dimensions.

In a large number of applications the magnetic field strength and flux density are fairly constant within a permanent magnet block (this is the case when an axially magnetized cylinder of arbitrary cross-section is located with its end faces against a high permeability material, as in the "basic" magnetic circuit of Fig. 2). For such problems the concepts load line and working point are helpful for rapid evaluation of permanent magnet fields [2].

The load line (see Fig. 1) is a straight line through origo, the slope of which is determined by the shape of the magnet and the configuration of the magnet assembly. The intersection of the load line with the demagnetization curve is the working point of the magnet ( $B_m$ ,  $H_m$ ). Reference [2] describes several ways of load line evaluation for different magnetic circuits. The simplest case consists of a bare magnet block in free space. Instead of a load line this case is frequently described by a "demagnetization factor", which is determined by the shape of the magnet.

In many cases the utilization of permanent magnet material is optimized if the working point coincides with  $(BH)_{\max}$ . The potential energy of the field outside the magnet is then maximized. This can be seen from the general expression of the magnetic energy:

$$W = \frac{1}{2} \int_{V_o} \vec{B} \cdot \vec{H} dV = -\frac{1}{2} \int_{V_m} \vec{B}_m \cdot \vec{H}_m dV \quad (1)$$

In Eq. (1)  $V_o$  is the field space outside the magnet and  $V_m$  is the magnet volume. The maximum magnetic energy of the outside field, which can be generated by a permanent magnet is thus simply:

$$W = \frac{1}{2} V_m \cdot (BH)_{\max} \quad (2)$$

The demagnetization curves of modern high coercivity materials are close to straight lines with the slope  $\mu_o$ . In such materials the magnetic polarization is rigid and close to  $B_r$  in the whole third quadrant and the magnetic field can often be calculated by integrating the dipole fields generated by volume elements of the magnet. The dipole strength (magnetic moment) of a volume element is then simply

$$d\vec{M} = \frac{1}{\mu_o} \vec{B}_r dV \quad (3)$$

In this case the field can also be calculated from an equivalent surface current or charge at the surface of the magnet [3]. This approach is especially favourable in the case of an axially magnetized straight cylinder, which is the preferred shape of magnet blocks in many applications. The equivalent "magnetic charge" density at the end surfaces is then simply  $= B_r$ . Alternatively a current of surface density  $B_r/\mu_o$  on the mantle surface generates the same field. Note that while both methods yields the correct field outside the magnet, only the equivalent charge gives the correct field strength inside the magnet and correspondingly the equivalent current sheet gives the correct interior flux density. When such high coercivity magnets are used together with yokes or poles of high permeability, many methods originally developed for the calculation of electrostatic fields (images, conformal mapping, variable separation and series approximations) can be utilized [4].

#### 4. ELECTROMAGNETS VERSUS PERMANENT MAGNETS

In principle most static or quasistatic fields required in accelerators can be generated either by electromagnets or permanent magnets. There are a number of factors influencing the choice, the most important of which are examined in some detail below.

##### 4.1 Field control

Field control of electromagnets is easily and effectively achieved by the use of variable current power supplies. With proper design of coils and power supplies a wide range from fast pulsed to stationary magnetic fields can be covered. In this respect permanent magnets are at a disadvantage. They are basically suited only for fixed field applications.

Field control of permanent magnet systems is, however, in many cases possible by moving iron or magnet parts with respect to each other. Such mechanical field control is necessarily always fairly slow and can be very complicated to implement. Further difficulties are generated by the magnetic forces between the moving parts, which can be very large. In planar insertion devices (see Section 6) peak field control is as a rule achieved by moving two magnet arrays symmetrically with respect to the field axis. In high field wigglers the magnetic force between these magnet arrays can reach several tens of tons.

## **4.2 Field stability**

The field stability of an electromagnet is generally related directly to the current stability of the power supply. The stability of modern magnet power supplies are typically better than 0.01 % and stabilities down to 1 ppm over an operating temperature range of 20 °C are available.

In permanent magnet systems the field stability is generally limited by the temperature coefficient of the remanence. As can be seen from Table 1 a temperature stability of 0.02 %/°C is the best that can be achieved and for the nowadays preferred NEO-materials the temperature stability is worse than 0.1 %/°C. This limits the use of permanent magnets to applications where stability is not critical. It is generally not feasible to stabilize the temperature of the magnets to better than about 0.5 °C, which results in a limit of 0.01 % for the field stability.

There are two ways in which the temperature stability of a permanent magnet assembly can be improved. One is based on combinations of soft magnetic materials and permanent magnets with temperature coefficients of different sign. This is a delicate procedure, which as a rule is feasible only in small systems such as instruments and not when fields must be generated in larger volumes, which is generally the case in accelerator magnets. Another possibility is the incorporation of a small correction electromagnet into the permanent magnet circuit. By controlling the current of this electromagnet with the aid of one or several temperature sensors mounted on the permanent magnet blocks, an improvement of the temperature stability of the field by up to a factor ten can be achieved, but only at the price of a much more complicated system.

## **4.3 Power consumption**

The great advantage of using permanent magnets is of course that they can sustain a static field without any power consumption. The power consumption of accelerator electromagnets can be considerable, but the power costs themselves are generally marginal. The power supplies and cooling systems of electromagnets do, however add a lot to the capital costs, space requirements and complexity of a complete electromagnetic setup. Cooling requirements also set a limit to the generation of certain spatially rapidly varying fields (e.g. in insertion devices, see Section 6) and in such cases permanent magnets offer the only solution.

#### 4.4 Radiation hardness

In high energy accelerators radiation damage can cause serious problems. In electromagnets coil insulations are the most susceptible materials. Electromagnet coils are on the other hand often naturally shielded by the heavy iron yokes and coils are generally not located very close to the high energy particle beams. In efficient permanent magnet circuits the magnets must, on the other hand, often be located fairly close to the region into which the useful field is generated. Most permanent magnets have excellent radiation resistance, but in NEO-magnets biased close to the coercivity partial demagnetization has been observed as the result of high energy ion radiation. The damage can in principle be repaired by remagnetization, but this often requires demounting of the magnetic assembly, which is generally difficult and often impossible.

#### 4.5 Field strength and field volume

The field strength and field volume (the spatial extent of space which the specified field must occupy) are important factors in the choice between different sources. In practice the saturation of iron restricts the useful flux density of both normal electromagnets and permanent magnet circuits in accelerator applications to values below 2 Teslas (except for some special cases of rapidly pulsed electromagnets). This restriction is of an economical/practical nature - in principle there is no limit to the field strength that can be generated by either method.

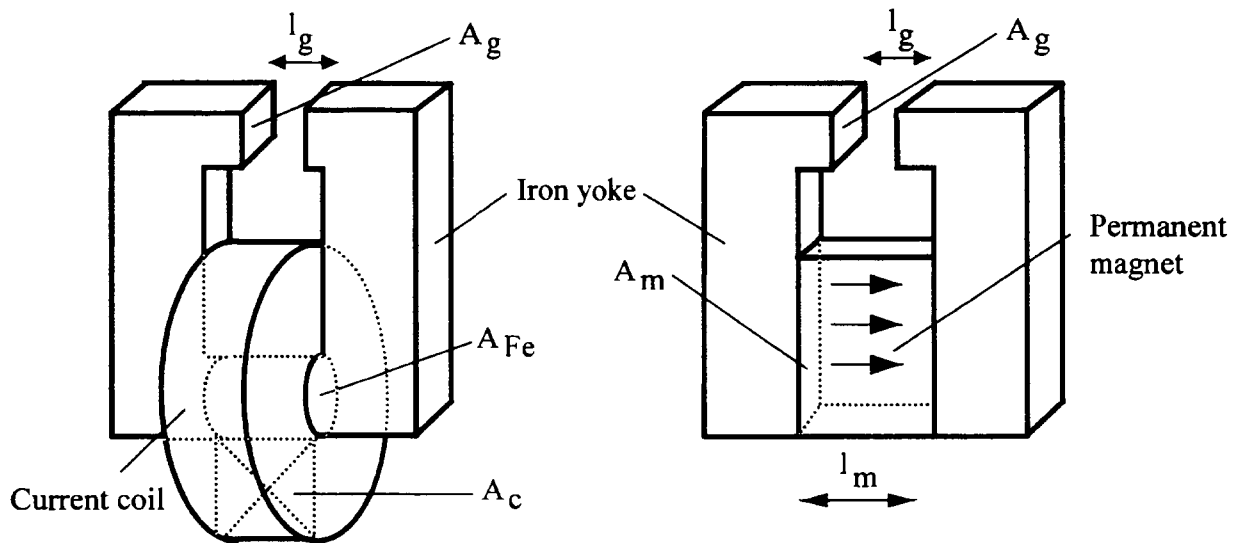


Fig. 2 A magnetic field can be generated in air gap  $A_g \times l_g$  with an electromagnet (left) or a permanent magnet (right).

In the range from 0 to 2 T the size and cost of electromagnets and permanent magnets scale differently with field strength and field volume. An analysis the "basic" magnetic circuits of Fig. 2 illustrates this fact. In both cases a field strength of  $H_g$  (a flux density of  $B_g = \mu_0 H_g$ ) shall be generated in an air gap of cross-sectional area  $A_g$  and width  $l_g$ . The exterior parts of the iron yokes are identical, iron losses are ignored and the leakage factor (ratio of total flux to air gap flux) is  $\sigma$ . For simplicity the coil cross-section (area  $A_c$ ) is assumed to be square and the air gap cubic (gap volume  $V_g = A_g l_g = l_g^3$ ).

If the circular coil aperture (cross-sectional area of the iron yoke at the coil location) is denoted  $A_{Fe}$ , it is easy to show that the volume of the ring-shaped coil can be expressed as

$$V_c = \pi A_c \left( \sqrt{A_c} + \frac{2}{\sqrt{\pi}} \sqrt{A_{Fe}} \right) \quad (4)$$

By definition the coil flux ( $B_{Fe}A_{Fe}$ ) is equal to the air gap flux ( $B_gA_g$ ) multiplied by the leakage factor. This determines the required coil aperture:

$$A_{Fe} = \frac{\sigma B_g A_g}{B_{Fe}} \quad (5)$$

$B_{Fe}$  denotes the maximum flux density allowed in the iron. The magnetomotive force of the coil (ampereturns), is equal to the potential drop across the air gap ( $NI = H_g l_g$ ). The maximum ampereturns that the coil can sustain are basically proportional to the cross-sectional area ( $NI = A_c$ ). The maximum current density ( $\alpha$ ) in the coil depends on the resistivity of the coil wire, the filling factor of the winding and the cooling method, but once these are fixed it tends to be fairly constant. The required coil cross-section is then:

$$A_c = \frac{H_g l_g}{\alpha} \quad (6)$$

By substituting Eqs. (5) and (6) into Eq. (4) an expression for the coil volume required to generate the gap field is obtained:

$$V_c = \left( \frac{\pi}{\alpha^2} V_g^{\frac{1}{2}} + \frac{2}{\alpha} \sqrt{\frac{\pi \sigma \mu_o}{B_{Fe}}} V_g^{\frac{2}{3}} \right) H_g^{\frac{3}{2}} \quad (7)$$

The total power consumption of the coil is also proportional to the volume.

The volume of the permanent magnet is simply  $A_m l_m$ .  $A_m$  is again determined by equating the magnet flux  $B_m A_m$  with the gap flux multiplied by the leakage factor:

$$A_m = \frac{\sigma B_g A_g}{B_m} \quad (8)$$

The magnetomotive force of the magnet is  $H_m l_m$  and again by equating this to the potential drop across the air gap  $l_m$  is obtained:

$$l_m = \frac{H_g l_g}{H_m} \quad (9)$$

By multiplying Eqs. (8) and (9) the amount of permanent magnet material needed to generate the gap field is found to be:

$$V_m = \frac{\sigma \mu_o}{B_m H_m} V_g H_g^2 \quad (10)$$

From Eq. (10) it is immediately obvious that the magnet volume is minimized if the magnet is shaped so that the working point  $(B_m, H_m)$  coincides with  $(BH)_{max}$ .

Comparison between Eqs. (7) and (10) shows the different scaling with size and field strength for electromagnets and permanent magnets. The amount of permanent magnet material needed to produce the specified field increases linearly with field volume and with the square of the field strength, while the coil size and power consumption of the electromagnet increases more slowly with both variables. It is consequently natural that permanent magnet applications become economically disadvantageous at high field strengths and volumes. The critical values at which permanent magnet solutions become uneconomical vary largely with the application. As a rule of thumb it can, however, be stated that permanent magnets are seldom economical for field volumes above a few  $dm^3$ .

Another important consequence of the different scaling laws follows directly from Eqs. (6) and (9). If all dimensions of a magnet assembly are scaled by the same factor, the field strength remains constant in the permanent magnet case, while at constant current density it scales proportionally to the dimensions in electromagnets. Small field volumes or spatially rapidly varying fields, can thus be very inconvenient to excite by electromagnets, because the size of the coils becomes excessive as compared to the field volume.

## 5. MULTIPOLE MAGNETS

The majority of all accelerator magnets fall into the category of "multipole magnets", the integrated fields of which have certain electron optical bending or focussing properties. Field control and stability criteria as a rule require that they are realized as electromagnets. In many cases field volumes are also too large for permanent magnet solutions. Nevertheless, permanent magnet multipoles have been implemented in accelerators in considerable quantities [5,6] in less demanding locations. Especially where small beam apertures suffice considerable space and cost savings can be possible.

Multipole magnets can be constructed with permanent magnets in much the same way as the traditional electromagnets, in which the field shape is determined by an iron yoke. There is, however, a much more efficient way to generate these fields with permanent magnets. Consider the ring-shaped area ( $r_1 < r < r_2$ ) in Fig. 3, which represents the cross-section of a hollow permanent magnet cylinder. The magnetic polarization of this high coercivity magnet has a fixed amplitude ( $B_r$ ), but its direction varies in the x-y plane according to:

$$\vec{J} = B_r e^{i\varphi(N+1)} \quad (11)$$

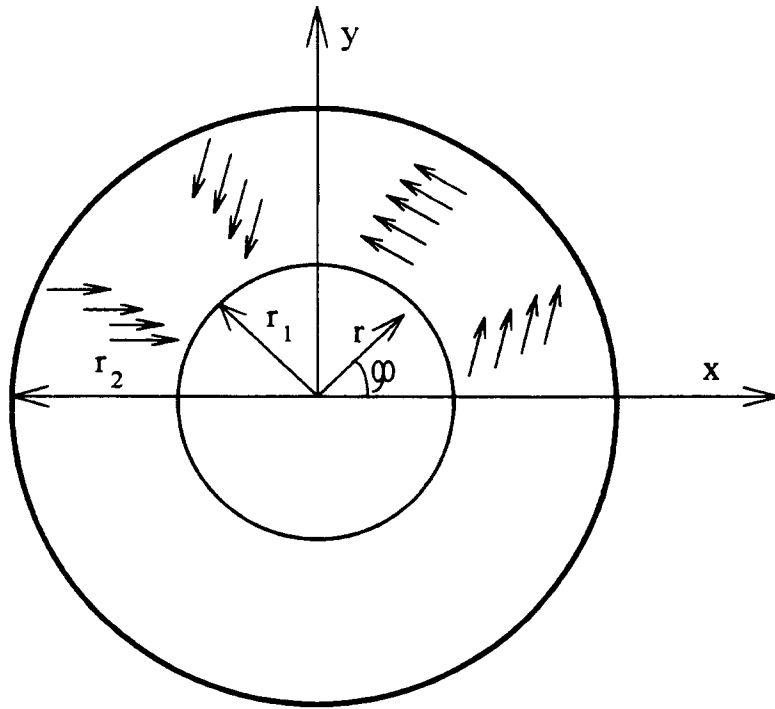


Fig. 3 Permanent magnet ring generating ideal multipole field. The magnetization amplitude is fixed but its direction varies with  $\varphi$ .

In Eq. (11)  $J = J_x + iJ_y$  is the complex polarization and  $N$  an arbitrary integer. It can be shown (7) that such a pattern of magnetization generates a field within the aperture  $r < r_1$ , the flux density of which is:

$$\bar{B} = B_r \left( \frac{\bar{z}}{r_1} \right)^{N-1} \cdot \frac{N}{N-1} \left[ 1 - \left( \frac{r_1}{r_2} \right)^{N-1} \right] \quad (12)$$

for  $N > 1$  and

$$\bar{B} = B_r \ln \left( \frac{r_2}{r_1} \right) \quad (13)$$

for  $N = 1$ . In Eqs. (12) and (13)  $B = B_x + iB_y$  is the complex flux density and  $z = x + iy$  the complex two-dimensional spatial coordinate. It can furthermore be shown that no magnetic field is generated outside the ring. It is readily seen that Eq. (12) represents a perfect multipole field and Eq. (13) a constant or dipole field. A permanent magnet, which is magnetized according to the pattern of Fig. 3 would thus constitute a perfect multipole magnet (dipole for  $N=1$ , quadrupole for  $N=2$ , sextupole for  $N=3$ , ...) with no stray field, provided the magnetic polarization remains rigid. High coercivity REC or NEO materials could in principle retain an almost constant polarization in such a configuration. Since these materials are anisotropic their easy direction would, however, also be required to vary spatially in the same way and this cannot in practice be achieved in rings of any significant thickness ( $r_2 - r_1$ ). Even in isotropic materials the magnetization of rings in the pattern of Fig. 3 is virtually impossible.

### 5.1 Segmented multipole magnets

The magnetization pattern of Fig. 3 can be approximated in a practical way by replacing the continuously magnetized ring with uniformly polarized wedge-shaped pieces as shown in Fig. 4. Such pieces can be cut out of larger magnet blocks to the desired shape. If the number of segments is  $M$  the polarization is rotated by  $\phi = 2\pi(N+1)/M$  from one segment to the next. The two-dimensional field within the aperture of such a segmented multipole magnet array can be calculated exactly as a Fourier series of multipole terms [7]:

$$\bar{B}(\bar{z}) = B_r \sum_{n=0}^{\infty} \left( \frac{\bar{z}}{r_1} \right)^{N+nM-1} \cdot \frac{N+nM}{N+nM-1} \left[ 1 - \left( \frac{r_1}{r_2} \right)^{N+nM-1} \right] \cdot K_n \quad (14)$$

For  $n=0$  and  $N=1$  the second factor in the sum of Eq. (14) is equal to  $\ln(r_2/r_1)$ . The third factor ( $K_n$ ) is given by:

$$K_n = \frac{M \cdot \cos^{N+nM}(\pi/M) \cdot \sin[\pi(N+nM)/M]}{\pi(N+nM)} \quad (15)$$

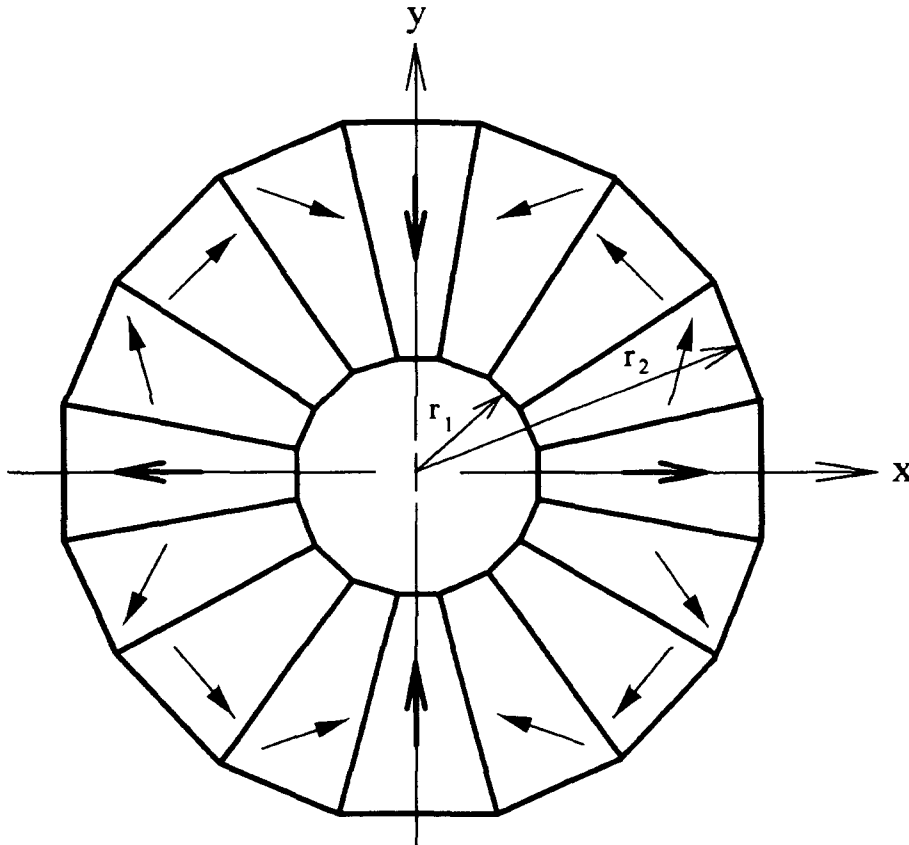


Fig. 4 Segmented quadrupole magnet

For the field outside the magnet assembly a corresponding series can be evaluated:

$$\bar{B}(\bar{z}) = B_r \sum_{n=1}^{\infty} \left( \frac{r_2}{\bar{z}} \right)^{nM-N+1} \cdot \frac{nM-N}{nM-N+1} \left[ 1 - \left( \frac{r_1}{r_2} \right)^{nM-N+1} \right] \cdot K_n' \quad (16)$$

The factor  $K_n'$  in Eq. (16) is given by:

$$K_n' = \frac{M \cdot \cos^{nM-N}(\pi/M) \cdot \sin[\pi(nM-M)/M]}{\pi(nM-N)} \quad (17)$$

The segmented multipole magnet does not produce a perfect multipole field of order  $N$ , but higher harmonics are present as well. If  $M$  is chosen large enough (in practice  $M \geq 8N$  is sufficient) the desired harmonic is dominating and other harmonics can be suppressed as much as wanted. The field outside the assembly then contains only high harmonics, which decay very rapidly with increasing distance, and the factors  $K_n$  and  $K_n'$  are close to 1.

As an example let us look at a quadrupole magnet for linac focussing. Such a magnet can have a very small aperture, 5 mm or less. IF the quadrupole is assembled of 16 NEO-magnet pieces with  $B_r = 1.2$  T,  $r_1 = 5$  mm and  $r_2 = 20$  mm, a gradient of 3.3 T/cm is achieved. This value would be very difficult to reach with a much larger electromagnet. Theoretically the lowest undesired harmonic ( $n=1$ ) is of order 18 and its amplitude is significant only very close to the outer edge of the aperture. In practice the relative permeability of NEO-magnet materials is not exactly 1, which leads to the appearance of harmonics of orders 6, 10 and 14 as well. In a real magnet inhomogeneities and mechanical imperfections produce even lower order stray harmonics, but the total content of undesired harmonics can be kept below 1 % of the quadrupole field within most of the aperture. The high aspect ratio ( $r_2/r_1$ ) of such an assembly has a serious consequence: Part of some of the segments are biased well into the third quadrant, which means that a very high coercivity material must be chosen to avoid partial demagnetization, which would cause severe degradation of the field. Locally the reverse field strength reaches 1300 kA/m, requiring that the coercivity of the polarization exceeds 1600 kA/m.

So far only the two-dimensional field near the centre of a long segmented multipole has been considered. Closer to the ends the field changes and there is also a fringe field reaching longitudinally outside the magnet. In accelerator multipole magnets the total steering effect can generally be evaluated as the longitudinal field integral. A remarkable property of segmented multipole magnets is the fact that this field integral at all locations within the aperture always is exactly the two-dimensional field multiplied by the magnet length. This is true even for very thin magnets, in which the local field at all longitudinal locations deviates significantly from the two-dimensional approximation. Magnet design can thus readily be based on Eqs. (14) - (17).

## 6. INSERTION DEVICES

There is a special class of accelerator magnets, the purpose of which is to give electrons or positrons a periodic lateral acceleration over some distance in the mean forward direction. Such insertion devices are employed to produce synchrotron radiation in a controlled manner (see chapters on synchrotron radiation and radiation damping in this publication). Insertion devices constitute the most important application of permanent magnets in accelerators. The field amplitudes (0.5 - 1.8 T) and periods (20 - 200 mm) typically required fall into the region in which permanent magnets are superior to electromagnets. If still higher peak fields are required superconducting magnets must be utilized.

Most insertion devices are of the planar type generating a periodic, generally almost sinusoidal field in a fixed direction, which is perpendicular to the particle beam trajectory. Special devices generate helical or asymmetric fields for the purpose of creating circularly polarized synchrotron radiation. This basic review is restricted to planar devices. An important parameter describing the working mode of an insertion device is the deflection factor given by:

$$K = \frac{qB_0 \lambda_u}{2\pi m_0 c} \approx 0.934 \cdot \lambda_u(\text{cm}) \cdot B_0(\text{T}) \quad (18)$$

where  $\lambda_u$  is the field period,  $B_0$  the maximum flux density (peak field),  $q$  the particle charge,  $m_0$  its mass and  $c$  the velocity of light. The insertion device is called a wiggler if  $K \gg 1$  and an undulator if  $K < 2-3$  (the limit is not sharp). The spectral properties and spatial distribution of synchrotron radiation produced by wigglers and undulators are radically different, but the magnet technology employed for building them is not influenced by this distinction. Reference [8] gives a more detailed overview of the theory of undulators and wigglers.

### 6.1 Undulator technology

The basic structures of permanent magnet undulators (and wigglers - what is said in this section about undulators generally holds for wigglers too) were developed by Halbach [9, 10] about 1980. Two magnet arrays with mirror symmetry are placed at opposite sides (usually below and above) of the particle trajectory. Figure 5 shows the two basic configurations of such arrays, generally referred to as the pure magnet configuration and the hybrid configuration. The peak field (and the deflection factor) can be varied by changing the gap between the two arrays. In practice most undulators are equipped with a mechanism allowing such "tuning" and also making it possible to shut off the device by increasing the gap until the field on axis becomes negligible.

The peak field of the pure magnet configuration can be calculated analytically as a function of the gap ( $g$ ), period ( $\lambda_u$ ), magnet block height ( $h$ ) and remanence of the magnet material ( $B_r$ ):

$$B_0 = \frac{4\sqrt{2}B_r}{\pi} e^{-\pi g/\lambda_u} (1 - e^{-2\pi h/\lambda_u}) \quad (19)$$

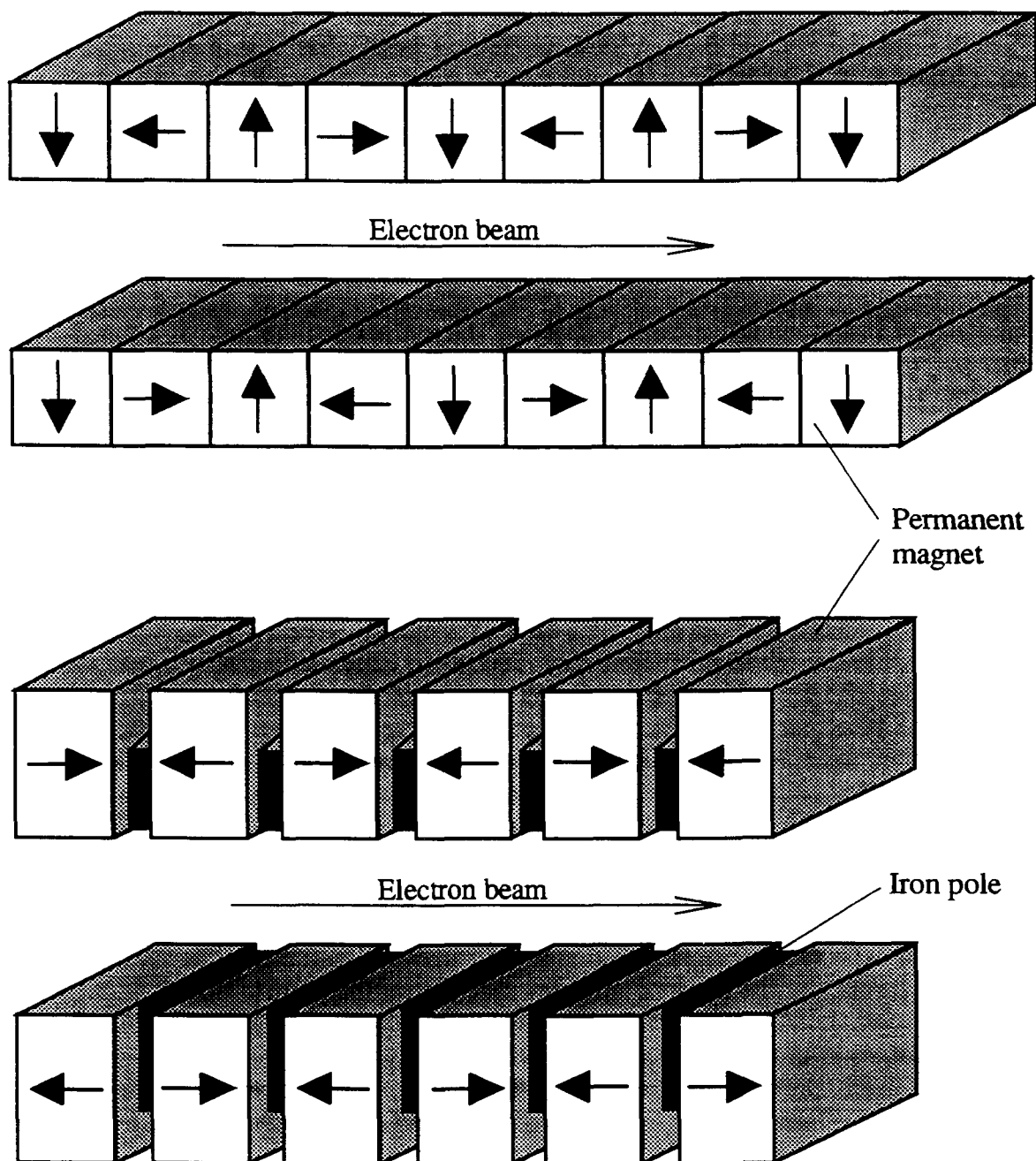


Fig. 5 Magnet configurations for planar insertion devices. The pure magnet configuration (top) employs eight magnet blocks per field period while the hybrid configuration (bottom) has four poles and four magnet blocks.

Equation (19) is actually a two-dimensional approximation valid for very wide magnet blocks. It is, however, common practice to choose wide enough blocks for Eq. (19) to give accurate results at least for the minimum gap. The block height ( $h$ ) varies between  $\lambda_u/4$  (square cross-section) and  $\lambda_u/2$ . Further increase contributes very little to the peak field as can readily be seen from Eq. (19).

The field of the hybrid configuration cannot be evaluated analytically. The number of variables are larger than in the pure magnet case and thus the optimum magnet and pole dimensions for a given period and gap can only be found by a trial and error procedure. For fixed dimensions the field is calculated by finite element or approximate analytical methods. Halbach has evaluated optimum hybrid dimensions for a large number of cases by two dimensional finite element calculations (wide poles and magnets). The results have been combined in a semi-empirical formulae, giving the achievable peak field as a function of the ratio  $g/\lambda_u$  [11]:

$$B_o = a \cdot e^{-\frac{g}{\lambda_u} \left( b - c \frac{g}{\lambda_u} \right)} \quad (20)$$

The constants in Eq. (20) are given by:  $a = 0.52B_r(T) + 2.693$ ,  $b = -1.95B_r(T) + 7.225$  and  $c = -1.3B_r(T) + 2.970$ . The expression is valid for  $0.07 < g/\lambda_u < 0.7$  and  $0.9 < B_r < 1.1$ . The simulations leading to Eq. (20) were based on a constant slope of the load line defining the working point of the bulk of the magnet. Theoretically this working point can always be achieved, but in practice it may require too large amounts of magnet material. A practical three-dimensional optimization of the hybrid configuration often leads to dimensions in which the pole height is larger than its width and then it is clear that a two-dimensional approximation assuming infinite width cannot be very reliable in predicting the field. Nevertheless, Eq. (20) is often referred to in evaluations of the hybrid configuration. The smaller the period the more realistic such evaluations are.

The inverse exponential dependence on the factor  $g/\lambda_u$ , which is a common feature of Eqs. (19) and (20), has serious consequences in undulator design. Often the period is fixed and then the achievable peak field varies steeply with the minimum allowable magnet gap. The gap is limited by the dynamic aperture required by the particle beam and the vacuum chamber design. It may be worth while to resort to very special and complicated vacuum chamber designs in order to gain a reduction of only a few millimeters in the minimum gap. In extreme cases the magnet arrays have been located in the vacuum, but due to the mechanical tuning needed and an often rather poor vacuum compatibility of permanent magnet materials this approach is generally avoided.

The choice of magnet configuration for a given undulator depends on several factors. We can use Eqs. (19) and (20) to compare the achievable peak field at a given ratio  $g/\lambda_u$ . For a NEO-magnet material with  $B_r = 1.1$  T we then get  $B_o = 1.59$  at  $g/\lambda_u = 0.07$  and  $B_o = 0.77$  T at  $g/\lambda_u = 0.3$  in the pure magnet configuration. For the hybrid configuration the corresponding peak fields are 2.31 and 0.82 T. If maximizing the peak field is important the hybrid configuration is thus superior. The difference decreases for increasing  $g/\lambda_u$  and when  $g/\lambda_u > 0.3$  the two configurations are almost equal in this respect. If a lower peak field is sufficient the amount of permanent magnet material needed is roughly the same for both configurations. The pure magnet configuration is then both conceptually and mechanically simpler. Field calculations and optimization procedures are also simpler than for the hybrid

configuration. On the other hand the high permeability poles of the hybrid configuration have a screening effect which reduces field errors on axis caused by inhomogeneities in the magnetization of the magnets. If a very high uniformity of the undulator field is required the hybrid configuration thus offers a better starting point. In many practical cases the choice of magnet configuration is, however, a marginal one, which tends to be resolved by institutional traditions and personal experience of the designer.

A more extensive review of undulator design and technology can be found in reference [12]. References [13] and [14] contain in depth treatment of many important aspects of undulator design and also a number of practical examples of constructed devices.

\* \* \*

## REFERENCES

- [1] K.J. Strnat, Proc. IEEE 78 (1990) 923.
- [2] R.J. Parker, Advances in permanent magnetism (John Wiley & Sons, 1990).
- [3] J.A. Stratton, Electromagnetic theory (McGraw-Hill, 1941).
- [4] K.J. Binns and P.J. Lawrenson, Analysis and computation of electric and magnetic field problems (Pergamon press, 1973).
- [5] K. Halbach, Nucl. Instr. and Meth. 187 (1981) 109.
- [6] R.F. Holsinger, Proc. 1979 Lin. Accel. Conf. Brookhaven BNL-51134 (1980) 373.
- [7] K. Halbach, Nucl. Inst. and Meth. 169 (1980) 1.
- [8] P. Elleaume, Proc. CAS Synchrotron Radiation and Free Electron Lasers CERN 90-03 (1990) 142.
- [9] K. Halbach, Journal de Physique 44 (1983) C1-211.
- [10] G. Brown et al., Nucl. Instr. and Meth. 208 (1983) 65.
- [11] E.S.R.F. Foundation Phase Report (1987) 314.
- [12] M. Poole, Proc. CAS Synchrotron Radiation and Free Electron Lasers CERN 90-03 (1990) 195.
- [13] R Tatchyn and I. Lindau ed., Proc. International Conference on Insertion Devices for Synchrotron Sources SPIE 582 (186).
- [14] I.H. Munro and D.J. Thomson ed., Proc. 4th International Conference on Synchrotron Radiation Instrumentation Rev. Sci. Instr. 63 (1992).